The EMBO Journal vol.14 no.2 pp.240–246, 1995

Electron microscopy of antibody complexes of influenza virus haemagglutinin in the fusion pH conformation

S.A.Wharton, L.J.Calder, R.W.H.Ruigrok[1], J.J.Skehel, D.A.Steinhauer and D.C.Wiley[2]

Division of Virology, MRC National Institute for Medical Research, Mill Hill, London, NW7 1AA, UK and [2]Department of Molecular and Cellular Biology, Howard Hughes Medical Institute, Harvard University, 7 Divinity Avenue, Cambridge, MA 02138, USA
[1]Present address: EMBL Grenoble Outstation, c/o ILL, PO Box 156, Grenoble Cedex 9, France

Communicated by J.Skehel

Activation of the membrane fusion potential of influenza haemagglutinin (HA) at endosomal pH requires changes in its structure. X-ray analysis of $TBHA_2$, a proteolytic fragment of HA in the fusion pH conformation, indicates that at the pH of fusion the 'fusion peptide' is displaced by >10 nm from its location in the native structure to the tip of an 11 nm triple-stranded coiled coil, and that the formation of this structure involves extensive re-folding or re-organization of HA. Here we examine the structure of $TBHA_2$ with the electron microscope and compare it with the fusion pH structure of HA_2 in virosomes, HA_2 in aggregates formed at fusion pH by the soluble, bromelain-released ectodomain BHA and HA_2 in liposomes with which BHA associates at fusion pH. We have oriented each HA_2 preparation for comparison, using site-specific monoclonal antibodies. We conclude that the structural changes in membrane-anchored and soluble HA preparations at the pH of fusion appear to be the same; that in the absence of a target membrane, the 'fusion peptide' of HA in virosomes associates with the virosome membrane so that HA_2 is membrane bound at both N- and C-termini, which implies that inversion of the re-folded HA can occur; and that the structural changes observed by X-ray analysis do not result from the proteolytic digestions used in the preparation of $TBHA_2$.

Key words: conformational change/electron miroscopy/ influenza virus haemagglutinin/membrane fusion/virus entry

Introduction

Influenza haemagglutinin (HA) membrane glycoproteins have two functions in the initial stages of virus infection. They bind viruses to cells by recognizing sialic acid residues of cell surface glycoconjugates and, following endocytosis, they mediate fusion of virus and endosomal membranes, allowing transfer of the genome–transcriptase complex into the cell (Wiley and Skehel, 1987). Membrane fusion activity requires changes in HA structure that are specifically induced at endosomal pH (between pH 5 and 6), and numerous studies involving antibody binding (Daniels *et al.*, 1983; Webster *et al.*, 1983; Yewdell *et al.*, 1983; White and Wilson, 1987), proteolytic fragment analyses (Skehel *et al.*, 1982; Ruigrok *et al.*, 1988), prediction of the fusion pH structure (Carr and Kim, 1993), site-specific mutation (Godley *et al.*, 1992) and experiments with mutants selected for differences in their pH of fusion (Daniels *et al.*, 1985, 1987) have provided information on the nature of the changes in structure. More directly, electron microscopy of HA at the pH of fusion (Ruigrok *et al.*, 1986) and of proteolytic fragments of HA in the fusion pH conformation (Ruigrok *et al.*, 1986, 1988), and X-ray crystallography of one of these fragments (Bullough *et al.*, 1994), have addressed the nature and extent of the structural changes. In this electron microscopic study of HA–antibody complexes, we compare the structures revealed microscopically with those from X-ray analysis and use the antibody probes to determine the orientation of membrane-anchored HA in the fusion pH conformation.

Native HA is a 220 kDa trimer of identical subunits, each of which consists of two disulphide-linked glycopolypeptides, HA_1 and HA_2. The structure of the soluble ectodomain (BHA) which is released from the virus membrane by bromelain digestion has been determined crystallographically to 2.2 Å resolution (Wilson *et al.*, 1981; Watowich *et al.*, 1994). It indicates that HA_1 glycopolypeptides primarily form a membrane-distal β-structure-rich globular domain containing the receptor binding sites, and that the major components formed by the HA_2 glycopolypeptide are a hairpin-like structure consisting of two anti-parallel α-helices of unequal length linked by a region of extended polypeptide chain, and a membrane-proximal 5-stranded β-sheet. The longer, 9 nm α-helices associate in the trimer to form a coiled coil along part of their length and then separate to accommodate the conserved hydrophobic N-terminal region of HA_2, the 'fusion peptide'. At the pH of fusion, soluble BHA forms aggregates as a consequence of the extrusion of the 'fusion peptide' (Skehel *et al.*, 1982). In this conformation, BHA is susceptible to proteolysis; digestion with trypsin releases HA_1 globular domains as monomers and subsequent digestion with thermolysin removes the 37 N-terminal residues of HA_2 including the 'fusion peptide' and solubilizes the residual aggregates, forming the trimeric fragment $TBHA_2$ (Ruigrok *et al.*, 1988; Bullough *et al.*, 1994). X-ray analyses of $TBHA_2$ crystals currently provide the only high-resolution structural data on HA in the fusion pH conformation (Bullough *et al.*, 1994). They show that the N-terminus of the thermolytic fragment, residue $HA_2$38, is displaced >10 nm from its location in the native molecule to the top of an ~11 nm long trimeric α-helical coiled coil. This structure is formed by the re-orientation in series of the shorter α-helix of the native α-helical hairpin, the extended chain which connects the

Table I. ELISA analyses of the binding of IIF4 and LC89 monoclonal antibodies to (A) different preparations of haemagglutinin and (B) different mutant haemagglutinins

Antigen	Monoclonal antibody	
	IIF4	LC89
(A) Haemagglutinin preparations		
X31 virus pH 7.0	<20	<20
X31 virus pH 5.0	2000	2560
BHA_2 aggregrates	16 000	5120
$TBHA_2$	16 000	5120
HA_2 38–125	<20	5120
(B) Mutant haemagglutinins		
X31 virus pH 5.0	1600	2560
$Q105_2K$ virus pH 5.4	1600	5120
$T107_2I$ virus pH 5.4	1600	320
$D112_2G$ virus pH 5.4	1600	5120
$E114_2K$ virus pH 5.4	1600	2560

The HA antigen preparations used were (A) X31 virus in PBS (pH 7.0); X31 virus in PBS (pH 5.0); BHA_2 aggregrates prepared by incubating soluble BHA at pH 5.0 followed by tryptic digestion (BHA:trypsin 50:1, 20°C, 30 min) to remove HA_1 residues 28–328; $TBHA_2$ prepared by digesting BHA_2 aggregrates with thermolysin at pH 5.0 (BHA_2:thermolysin 50:1, 37°C, pH 5.0, 6 h) to remove BHA_2 residues 1–37; HA_2 38–125 prepared by digesting BHA_2 aggregrates with thermolysin at pH 8.4 (BHA_2:thermolysin 50:1, 37°C, pH 8.4, 6 h) to remove BHA_2 residues 1–37 and 126–175. (B) X31 virus and HA mutants of X31 which fuse membranes at higher pH than wild type. Viruses were incubated at either pH 5.0, X31, or pH 5.4, mutant viruses, and then with trypsin (virus:trypsin 100:1, 20°C, 30 min) to remove HA_1 residues 28–328. The amino acid substitutions in the mutant HAs are used to name the mutants, e.g. mutant $Q105_2K$ contains lysine substituted for glutamine at residue HA_2 105. The ELISA procedure is described in Materials and methods. The values given are the reciprocals of the highest dilution of antibody scored as positive.

two α-helices now re-folded into an α-helix and the N-terminal 30 residues of the longer α-helix which also formed a coiled coil in the native molecule. At the C-terminal end of each helix of this coiled coil, seven residues of the native longer α-helix re-fold to form a turn which displaces the remainder of the α-helix, and the C-terminal structural elements of HA_2 and HA_1 associated with it, through 180°. The C-terminal 13 residues appear to be disordered.

In attempts to obtain information on the structural location of this C-terminal region and to investigate the contributions of the HA membrane anchor and the 'fusion peptide' to the conformation of HA at the pH of fusion, we have examined electron microscopically different preparations of HA in the fusion pH conformation and have compared the images obtained with the X-ray structure of $TBHA_2$. We have analysed, in particular, HA in virosomes incubated at the pH of fusion, fusion pH-induced aggregates of BHA, and liposomes formed by dialysis of BHA, detergent, and lipid mixtures at the pH of fusion, as well as complexes of all of these preparations with monoclonal antibodies which react specifically with HA_2 in the fusion pH conformation.

Results

Determination of antibody specificities

The principal monoclonal antibody used, LC89, reacts in enzyme-linked immunosorbent assay (ELISA) (Table IA)

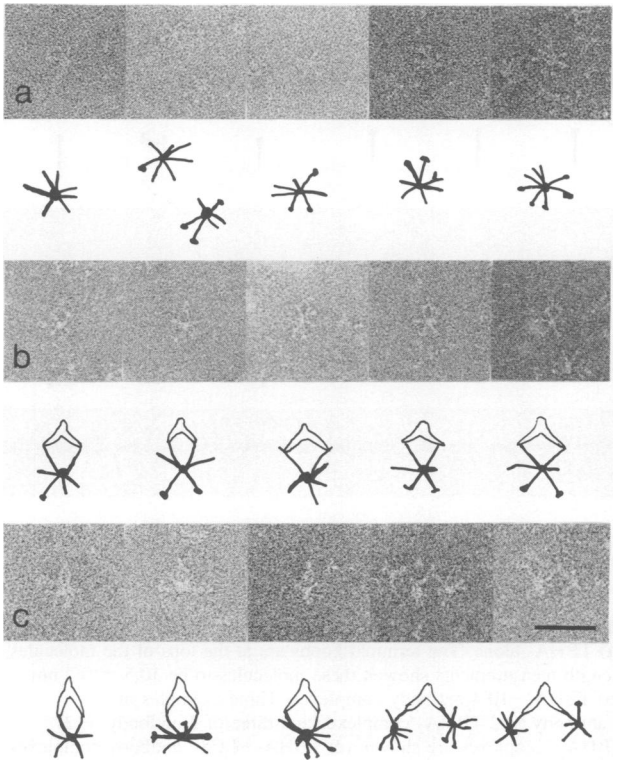

Fig. 1. Electron micrographs of BHA_2 aggregate–antibody complexes. (**a**) BHA_2 aggregates alone. Diagrammatic representations of the molecules are shown below each micrograph. (**b**) BHA_2 aggregate–IIF4 antibody complexes. In the diagrams the antibodies are shown as open shapes. (**c**) BHA_2 aggregate–LC89 antibody complexes. Bar ≡ 50 nm.

specifically with HA in the fusion pH conformation and with $TBHA_2$. The other antibody, IIF4 (Vareckova *et al.*, 1993), also binds to $TBHA_2$, but not to a smaller fragment of HA_2 which lacks the 50 C-terminal residues of $TBHA_2$. The inability of either antibody to bind to native HA (Table IA) precludes the selection of antigenic variants to obtain finer definition of their binding specificity from variant sequencing studies. However, we have attempted to obtain similar information by assessing the ability of the antibodies to bind to mutant HAs selected to fuse membranes at higher pH than wild type, which we have shown to contain a variety of single amino acid substitutions (Daniels *et al.*, 1985). The results in Table IB indicate that whereas antibody IIF4 binds to all mutant HAs tested, LC89 binds significantly less well to a mutant HA containing a threonine to isoleucine substitution at HA_2107. In the X-ray structure of $TBHA_2$ (Bullough *et al.*, 1994), HA_2107 is located at one end of the $TBHA_2$ trimer in the turn formed by the re-folded native α-helical residues HA_2 106–113.

Electron microscopy of HA_2 in the fusion pH conformation

At the pH of fusion, BHA aggregates through extrusion of the conserved, hydrophobic amino terminal region of HA_2, the 'fusion peptide' (Skehel *et al.*, 1982). Digestion with trypsin removes HA_1 residues 28–328, leaving BHA_2 aggregates. Both types of aggregate have been analysed before by electron microscopy (Ruigrok *et al.*, 1986).

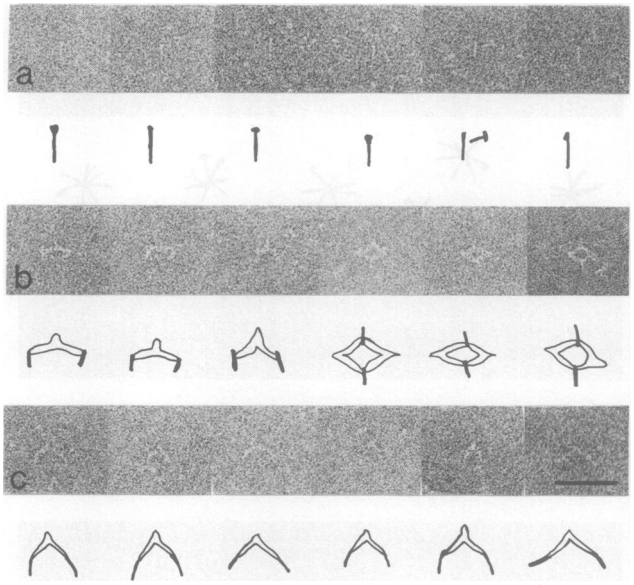

Fig. 2. Electron micrographs of $TBHA_2$–antibody complexes. (**a**) $TBHA_2$ alone. The terminal knobs are at the tops of the molecules. Length measurements showed these molecules to be 10.5 ± 0.7 nm. (**b**) $TBHA_2$–IIF4 antibody complexes. Three examples of 1 antibody + 2 $TBHA_2$ complexes and three of 2 antibody + 2 $TBHA_2$ complexes are shown. (**c**) $TBHA_2$–LC89 antibody complexes. Complexes of 1 antibody + 2 $TBHA_2$ are shown; none greater was observed. In the diagrams the antibodies are shown as open shapes. Bar ≡ 50 nm.

Micrographs of BHA_2 aggregates are shown in Figure 1a and $TBHA_2$, prepared from them by digestion with thermolysin, in Figure 2a. The diameter of the aggregates indicates a BHA_2 minimum length of 15 nm and many of the spikes had knobs at their projected ends. $TBHA_2$ molecules were 11 nm long and the majority had knobs at one end. Liposome-associated BHA_2 (Figure 3a), a preparation formed following dialysis to remove detergent from mixtures of fusion pH BHA, detergent and lipids, and then removal of HA_1 from the membrane-associated BHA by tryptic digestion, had similar dimensions to $TBHA_2$ in projecting ~11 nm from the membrane surface and, in many cases, having knobs at their membrane-distal ends. Thermolytic digestion of the liposomes released a soluble fragment indistinguishable in molecular weight from $TBHA_2$ by PAGE (Figure 4) and with the same N-terminal sequence as $TBHA_2$, indicating that lipid association of BHA_2 in these preparations was via the 'fusion peptide'. Figure 5a shows micrographs of HA_2 in the fusion pH conformation projecting from virosomes. Following incubation of virosomes containing HA at the pH of fusion, HA_1 residues 28–328 were removed by tryptic digestion and, as reported before (Ruigrok *et al.*, 1986), the HA_2 spikes project perpendicularly from the membranes with a length of ~11 nm and the majority had a membrane-distal knob.

Electron microscopy of HA_2–antibody complexes

The micrographs shown in Figures 1, 2, 3 and 5 also contain images of the above HA_2 preparations complexed with monoclonal antibodies IIF4 or LC89.

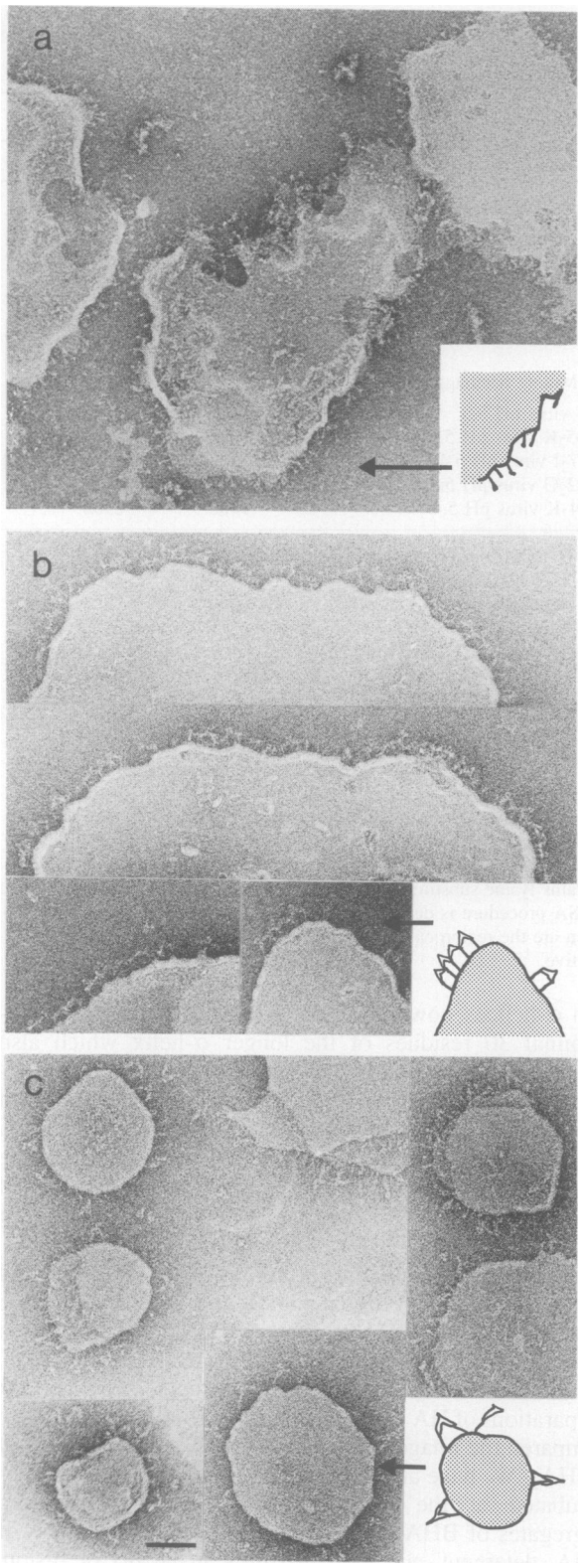

Fig. 3. Electron micrographs of liposome-associated BHA_2–antibody complexes. Liposomes were digested with trypsin to remove HA_1 28–328 as described in Materials and methods. (**a**) Liposome-associated BHA_2 alone. The BHA_2 spikes are 11.4 ± 1.6 nm long. (**b**) Complexes with IIF4 antibody. (**c**) Complexes with LC89 antibody. The insets are diagrams of the liposomes arrowed. Bar ≡ 50 nm.

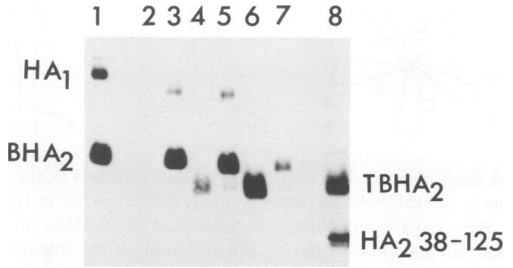

Fig. 4. The thermolytic release of $TBHA_2$ from liposome-associated BHA_2. Liposome-associated BHA_2 prepared as described in Materials and methods was digested with thermolysin [PBS (pH 6.0), 2 mM $CaCl_2$] at 37°C for 30 or 120 min. Digestion products were centrifuged at 100 000 *g* for 20 min, and the supernatant and pelleted material analysed by PAGE under reducing conditions. The separated polypeptides were detected by immunoblotting using an anti-HA rabbit antiserum. Lane 1, BHA marker; lanes 2, 4 and 6, supernatants from 0, 30 and 120 min digestions; lanes 3, 5 and 7, pellets from 0, 30 and 120 min digestions; lane 8, $TBHA_2$ marker preparation containing a small amount of the HA_2 38–125 fragment.

Complexes with antibody IIF4

Antibody IIF4 interacts with BHA_2 aggregates near the radially projected ends of the spikes, suggesting that it binds at the opposite end of the molecule to the 'fusion peptides' which associate centrally to form the aggregates (Figure 1b). This antibody binds at an angle of ~105° near one end of $TBHA_2$, but distinctly removed from it (Figure 2b). In this position, because the $TBHA_2$ trimer contains three non-overlapping antibody-binding sites, the formation of 2 antibody and 2 $TBHA_2$ (Figure 2b), and greater, complexes is observed.

With liposome-associated BHA_2, antibody IIF4 interacts near the membrane-distal end, again the opposite end to the lipid-bound 'fusion peptide' (Figure 3b); with HA_2 in virosomes it also binds near the membrane-distal ends of the spikes (Figure 5b). This last observation suggests that at fusion pH HA_2 associates with virosome membranes through both its C-terminal membrane anchor and its N-terminal 'fusion peptide'.

Complexes with antibody LC89

Antibody LC89 binds at the radially projected ends of aggregated BHA_2 (Figure 1c), opposite from the centre of the protein–protein micelles where the 'fusion peptides' are associated. This is consistent with mutant binding data (Table IB), which suggest that the binding site for LC89 includes residue $HA_2$107 at the opposite end of $TBHA_2$ to that from which the 'fusion peptide' has been proteolytically removed (Bullough *et al.*, 1994). This antibody binds on one end of $TBHA_2$, almost in line with the molecule, at an angle of 160°. In this position, near the three-fold axis of symmetry of $TBHA_2$, the three antibody-binding sites overlap and sterically only one antibody can be accommodated; complexes of 1 antibody + 2 $TBHA_2$ can form, but none greater is detected. This property is reminiscent of those anti-HA antibodies shown to bind at the membrane-distal tip of BHA which are also restricted to a maximal complex size of 1 antibody + 2 BHA (Wrigley *et al.*, 1983a).

Finally, antibody LC89 binds at the membrane-distal ends of both liposome-associated BHA_2 (Figure 3c) and HA_2 in virosomes (Figure 5c), providing strong support

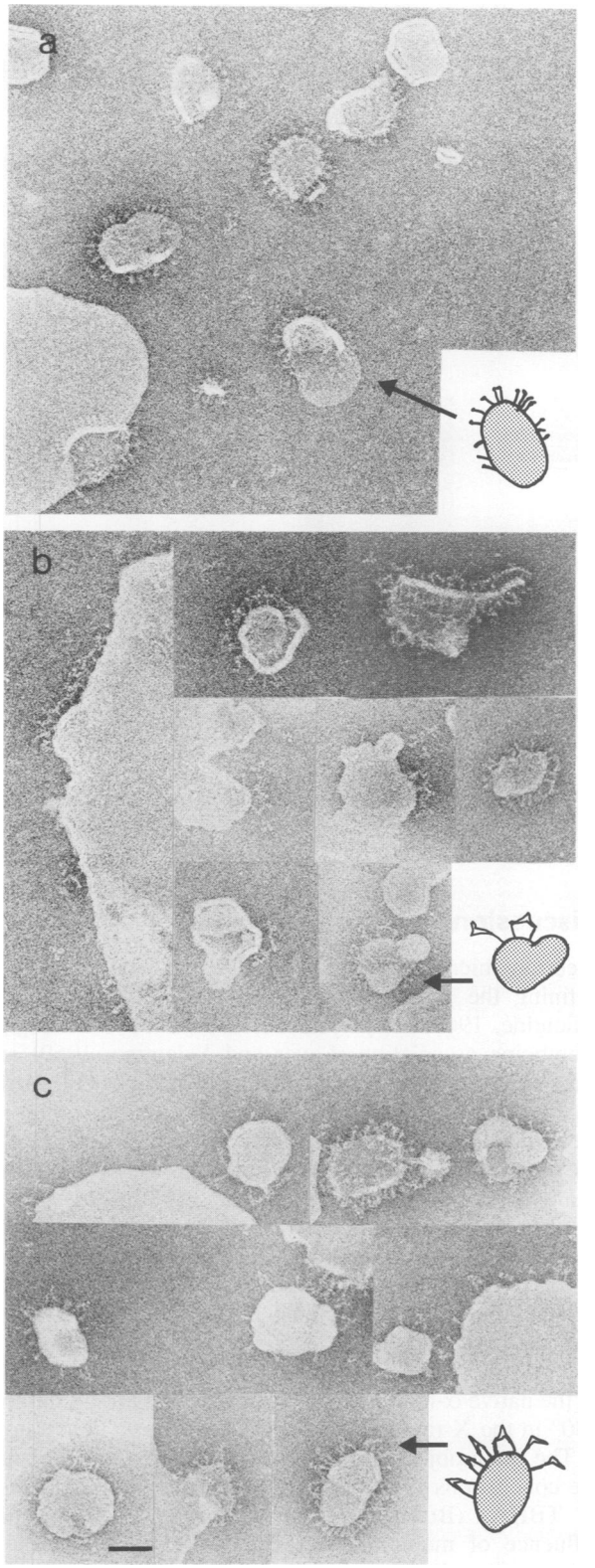

Fig. 5. Electron micrographs of virosome–antibody complexes. Virosomes were incubated at pH 5.0 and digested with trypsin to remove HA_1 28–328 as described in Materials and methods. (**a**) Virosomes alone. The HA_2 spikes were 11.3 ± 0.8 nm in length. (**b**) Virosomes incubated with IIF4 antibody. (**c**) Virosomes incubated with LC89 antibody. The insets are diagrams of the arrowed virosome and virosome–antibody complexes. Bar ≡ 50 nm.

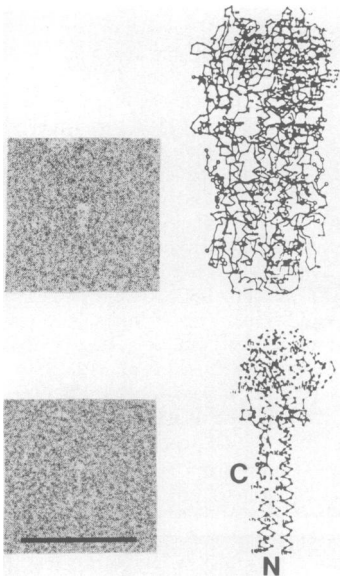

Fig. 6. A comparison of the EM and X-ray structures of BHA (upper) and $TBHA_2$. The EM images were reported in Ruigrok *et al.* (1986, 1988), and the X-ray structures in Wilson *et al.* (1981) and Bullough *et al.* (1994). Bar ≡ 50 nm. The locations of the N- and C-termini of $TBHA_2$ are indicated.

for the suggestion made from the results with antibody IIF4 that HA_2 is anchored in virosome membranes at both its N- and C-termini.

Discussion

Electron microscopy has been of considerable value in defining the shape and dimensions of HA (Laver and Valentine, 1969; Wrigley *et al.*, 1986), understanding its membrane association (Laver and Valentine, 1969) and mapping the regions to which infectivity neutralizing antibodies bind (Wrigley *et al.*, 1983a). In this study of the structure of HA_2 in the fusion pH conformation, as in previous comparisons of electron microscope and X-ray analyses of BHA (Ruigrok *et al.*, 1986), the images revealed microscopically are consistent with the recently determined X-ray structure of $TBHA_2$. Figure 6 compares electron micrographs of BHA and $TBHA_2$ with their molecular profiles determined by X-ray crystallography, and suggests that the knobs observed microscopically at one end of $TBHA_2$ correspond to the C-terminal region of the native α-helix, which is shown to be turned through 180° in the X-ray structure (Bullough *et al.*, 1994).

The main objective of the present study was to extend the conclusions drawn from the crystallographic analysis of $TBHA_2$ (Bullough *et al.*, 1994) by assessing the influence of membrane association on the structure of HA_2 at the pH of fusion and to correlate the electron microscope structures of HA_2 in virosomes observed previously with the structural information provided by the crystallographic study.

Our conclusions from analysing different preparations of HA_2 in the fusion pH conformation, complexed with monoclonal antibodies of defined specificity, are that: (i) the structures of $TBHA_2$ and membrane-associated HA_2 in virosomes are indistinguishable in the electron microscope,

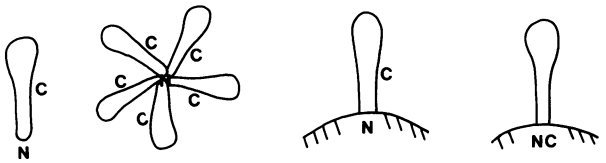

Fig. 7. A diagrammatic representation of the orientations of the HA fragments in the different preparations analysed. From left to right: $TBHA_2$; BHA_2 aggregates; liposome-associated BHA_2; HA_2 in virosomes. The locations of the N- and C-termini of the fragments are indicated.

implying that there are no gross structural consequences of the lack of a C-terminal membrane anchor for the conformation of HA at the pH of fusion; (ii) the two ends of the molecules defined in BHA_2 aggregates, in liposome-associated BHA_2 and in $TBHA_2$ are the same as those revealed crystallographically, i.e. one end is formed by the 'fusion peptide' or the N-terminal region from which it was removed by thermolysin, the other is formed by the turn resulting from the re-folding of HA_2 residues 106–113; and (iii) the 'fusion peptide' of HA in virosomes, on extrusion at the pH of fusion, associates with the virosome membrane so that HA_2 is membrane bound at both N- and C-termini, consistent with recent reports of photoactivated phospholipid labelling of HA in virus membranes (Weber *et al.*, 1994).

These conclusions, which are illustrated diagrammatically in Figure 7, are based on the interpretation of two experimental procedures which we have documented previously (Wrigley *et al.*, 1983a; Ruigrok *et al.*, 1988). The first is that thermolysin selectively removes the 'fusion peptide' from HA_2 in the fusion pH conformation. We have used this reaction before to prepare $TBHA_2$ from aggregated BHA and we use it here to show that BHA associates with liposomes through the 'fusion peptide'. The structural interpretation of these observations is that 'fusion peptides' form the centre of fusion pH-induced BHA_2 aggregates and are membrane proximal in fusion pH-induced liposome-associated BHA_2. By contrast, the monoclonal antibodies which we have used to orient the images bind to the opposite end of BHA_2 in these preparations. They also bind to one end of $TBHA_2$—that containing the knob structures seen electron microscopically—supporting the interpretation that this is opposite to the 'fusion peptide' end of the molecule.

The second experimental procedure concerns the definition of monoclonal antibody specificity, which is based mainly on estimates of antibody binding to mutant HAs containing single amino acid differences from wild type. The mutants used in this case were selected before (Daniels *et al.*, 1985), not as antigenic mutants, but for their ability to fuse membranes at higher pH than wild-type HA. However, on the assumption that amino acid substitutions cause primarily local changes in structure, we use them here to define the site of monoclonal antibody LC89 binding. This assumption is based on studies of antigenic variant HAs (Daniels *et al.*, 1983), electron microscopy of antibody–HA complexes (Wrigley *et al.*, 1983a), X-ray crystallography of variant HAs (Knossow *et al.*, 1984) and X-ray crystallography of HA fragment–Fab complexes (Bizebard *et al.*, in preparation) which have shown that the sites of amino acid substitution in antigenic variant HAs define the sites of antibody binding. Since

antibody LC89 binds comparatively poorly to the $T107_2I$ mutant HA, we conclude that residue HA_2107 at one end of $TBHA_2$ is included in its binding site. This is consistent with the observations that there is effectively only one binding site for antibody LC89 near the 3-fold axis of symmetry of $TBHA_2$, and with the discussion above of the structures and orientation of BHA_2 in aggregates and associated with liposomes.

A structural requirement of the conclusions that in virosomes both the 'fusion peptide' and the membrane anchor hold HA_2 in the membrane, and that the membrane-distal end is formed by the turn containing HA_2 107, is that the C-terminal region of HA_2 preceding the membrane anchor should be sufficiently flexible to allow the 11 nm long, fusion pH-induced coiled coil either to project towards the target membrane or to rotate back towards the virosome membrane in the absence of a target membrane. In the $TBHA_2$ X-ray structure this appears to be the case (Bullough *et al.*, 1994). Alternatively, the mechanism of fusion could require an exclusive interaction of the 'fusion peptide' with the virus membrane achieved by this rotation (or by a different process of re-folding perhaps involving uncoiling of the native coiled coil), but how such an interaction could mediate membrane fusion is not clear. As discussed before (Bullough *et al.*, 1994), insertion of 'fusion peptides' into virus membranes may be the basis for infectivity inactivation at low pH.

The consequences of our observations for the role of HA in membrane fusion primarily relate to the assocation of the 'fusion peptide' with membranes. Micrographs of liposome-associated BHA_2 and of HA_2 in virosomes both indicate a projecting length of 11 nm, no longer than $TBHA_2$, suggesting since the length of BHA_2 is ~15 nm (Figure 2) that the 'fusion peptide' and perhaps the N-terminal 37 residues that are removed in preparing $TBHA_2$ are buried in the liposome or virosome membranes, or interact with them along their surface. The information obtained from neither preparation is exactly that required for assessment of the interaction of a membrane-anchored HA with a sialic acid receptor-containing target membrane in the process of membrane fusion and attempts at such analyses are in progress. Nevertheless since the inserted molecules appear perpendicular to the membranes, they may project similarly from a target membrane. If this is the case, then flexibility in the C-terminal region of HA_2 alone may be insufficient to allow bending of the bridging spikes, which would seem to be required for close apposition, preceding fusion of virus and target membranes.

Finally, this study does not address the location of HA_1 which, at the pH of fusion, remains disulphide linked to HA_2. However, the observations that the monoclonal antibodies LC89 and IIF4 bind to intact HA in the fusion pH conformation (Table I) indicate that the fusion pH-induced structural changes are not restricted by the presence of HA_1 and that they do not result from its proteolytic removal.

Materials and methods

Virus and HA preparations

X31 and X31 mutant viruses (H3N2) were grown in embryonated eggs and purified as described previously (Skehel and Schild, 1971). BHA was released from virions by digestion with the protease bromelain and purified by sucrose gradient sedimentation as described previously (Brand and Skehel, 1972). BHA_2 aggregates were prepared by incubating BHA at pH 5.0 and 37°C for 10 min, neutralizing with 1 M Tris buffer (pH 8.0), and digesting the resulting BHA aggregates with trypsin (BHA:trypsin 50:1, w/w) at 20°C for 30 min. The BHA_2 aggregates were then purified by sucrose gradient centrifugation (Skehel *et al.*, 1982). $TBHA_2$ was made by digesting BHA_2 aggregates with the protease thermolysin (BHA_2:thermolysin 50:1, w/w) at pH 5.0 and 37°C, for 6 h (Ruigrok *et al.*, 1988). Virosomes were made as described previously (Ruigrok *et al.*, 1986) except that a synthetic lipid mixture (phosphatidylcholine : phosphatidylethanolamine : sphingomyelin : phosphatidylserine:phosphatidylinositol:cholesterol at molar ratios of 10:3:3:1:0.5:10) was used. A lipid–HA ratio of 30:1 (w/w) was used to give virosomes which were sparsely covered with HA to facilitate electron microscopic observation. Virosomes were incubated at pH 5.0 and digested with trypsin as described for the BHA_2 aggregates. BHA in the fusion pH conformation associated with lipid vesicles was made by mixing 5 mg of the lipid mixture described above with 0.5 mg BHA in phosphate-buffered saline (PBS; pH 7.4) containing 20 mM deoxy-BIGCHAP (Boehringer Mannheim). The pH was adjusted to pH 5.0 with 0.15 M citrate buffer (pH 3.5) and the mixture incubated at 37°C for 10 min. After neutralization with 1 M Tris buffer (pH 8.0), the preparation was dialysed extensively against multiple 5 l volumes of PBS containing Amberlite XAD-2 hydrophobic beads to accelerate the removal of the detergent. Trypsin digestion was as described above for the BHA_2 aggregates.

The HA_2 38–125 fragment was made by digestion of BHA_2 aggregates with thermolysin (BHA:thermolysin 50:1, w/w) at 37°C for 6 h in PBS (pH 8.4) containing 1 mM $CaCl_2$. The reaction was stopped by the addition of 10 mM EDTA. These conditions, in particular pH 8.4, were found to be optimal for the production of this fragment. The HA_2 38–125 fragment was purified by centrifugation at 100 000 *g* for 30 h at 20°C on a 2.5–15% sucrose gradient. Amino-terminal sequencing showed that the amino terminus of this fragment was the same as that of $TBHA_2$, i.e. HA_2 L38. Mass spectroscopy gave a subunit mol. wt of 10 410 Da, compatible with the carboxy terminus being HA_2 Q125. This fragment, therefore, also differs from $TBHA_2$ in lacking HA_1 1–27, which is disulphide bonded to HA_2 137 in $TBHA_2$ and all three oligosaccharide side chains present in $TBHA_2$.

Thermolysin treatment of lipid-associated BHA_2

Thermolysin digestion was carried out in PBS (pH 6.0) containing 2 mM $CaCl_2$. The digestion was stopped by the addition of 10 mM EDTA and the preparations were centrifuged at 100 000 *g* for 20 min in a Beckman TL100 centrifuge. Supernatants and pellets were analysed by PAGE under reducing conditions using 16% polyacrylamide gels, and the HA proteins were detected by immunoblotting using a polyclonal anti-BHA rabbit antiserum and the ECL detection system (Amersham).

Electron microscopy

Samples were absorbed onto carbon films and negatively stained with 1% sodium silicotungstate (pH 7.0). Micrographs were taken under minimum dose and accurate defocus conditions to preserve detail to ~1.5 nm (Wrigley *et al.*, 1983b). The JEOL 1200 EX microscope was operated at 100 kV and magnification was regularly calibrated with catalase crystals. A graticule eyepiece with ×10 additional magnification was used for the length measurements.

Antibody-binding experiments

The mouse monoclonal antibody IIF4 was a gift of Dr E.Vareckova and was raised against A/Dunedin/4/73 virus (H3N2) (Vareckova *et al.*, 1993). The antibody was purified from ascitic fluid using a protein A–Sepharose column (Pharmacia). The mouse monoclonal antibody LC89 was raised in CBA mice against detergent-extracted X31 HA in the fusion pH conformation as described previously (Daniels *et al.*, 1983). Antibody was purified from tissue culture supernatants by ammonium sulphate precipitation, followed by affinity chromatography using a protein A–Sepharose column. The antibody was of the IgG_1 subtype. In the electron microscopic studies, antibodies were incubated with the different HA preparations in PBS (pH 7.4) for 2 h at 20°C. The amount of antibody was adjusted to give the maximum number of antigen–antibody complexes. ELISA was carried out as described previously (Bos *et al.*, 1981) using goat antimouse antibody–peroxidase conjugate (Biorad) and 3,3′,5,5′ tetramethylbenzidine as substrate.

Acknowledgements

We thank Alan Douglas, Rose Gonsalves and David Stevens for excellent technical assistance, Alan Harris for amino acid sequencing. and Steve Howell and Alastair Aitken for mass spectroscopy. This work was supported by the MRC and NIH (A1-13654 to D.C.W.). D.C.W. is an investigator with the Howard Hughes Medical Institute.

References

Bos,E.S., Van der Doelen,A.A., Van Rody,N. and Schuurs,A.H.W.M. (1981) *J. Immunoassay*, **2**, 187–204.

Brand,C.M. and Skehel,J.J. (1972) *Nature New Biol.*, **238**, 145–147.

Bullough,P.A., Hughson,F.M., Skehel,J.J. and Wiley,D.C. (1994) *Nature*, **371**, 37–43.

Carr,C.M. and Kim,P.S. (1993) *Cell*, **73**, 823–832.

Daniels,R.S., Douglas,A.R., Skehel,J.J. and Wiley,D.C. (1983) *J. Gen. Virol.*, **64**, 1657–1662.

Daniels,R.S., Downie,J.C., Hay,A.J., Knossow,M., Skehel,J.J., Wang,M.L. and Wiley,D.C. (1985) *Cell*, **40**, 431–439.

Daniels,R.S., Jeffries,S., Yates,P., Schild,G.C., Rogers,G.N., Paulson,J.C., Wharton,S.A., Douglas,A.R., Skehel,J.J. and Wiley,D.C. (1987) *EMBO J.*, **6**, 1459–1465.

Godley,L. *et al.* (1992) *Cell*, **68**, 635–645.

Knossow,M., Daniels,R.S., Douglas,A.R., Skehel,J.J. and Wiley,D.C. (1984) *Nature*, **311**, 678–680.

Laver,W.G. and Valentine,R.C. (1969) *Virology*, **38**, 105–119.

Ruigrok,R.W.H., Wrigley,N.G., Calder,L.J., Cusack,S., Wharton,S.A., Brown,E.B. and Skehel,J.J. (1986) *EMBO J.*, **5**, 41–49.

Ruigrok,R.W.H., Aitken,A., Calder,L.J., Martin,S.R., Skehel,J.J., Wharton,S.A., Weis,W. and Wiley,D.C. (1988) *J. Gen. Virol.*, **69**, 2785–2795.

Skehel,J.J. and Schild,G.C. (1971) *Virology*, **44**, 396–408.

Skehel,J.J., Bayley,P.M., Brown,E.M., Martin,S.R., Waterfield,M.D., White,J.M., Wilson,I.A. and Wiley,D.C. (1982) *Proc. Natl Acad. Sci. USA*, **79**, 968–972.

Vareckova,E., Mucha,V., Ciampor,F., Betakova,T. and Russ,G. (1993) *Arch. Virol.*, **130**, 45–56.

Watowich,S.J., Skehel,J.J. and Wiley,D.C. (1994) *Structure*, **2**, 719–731.

Weber,T., Paesold,G., Galli,C., Mischler,R., Semenza,G. and Brunner,J. (1994) *J. Biol. Chem.*, **269**, 18353–18358.

Webster,R.G., Brown,L.E. and Jackson,D.C. (1983) *Virology*, **126**, 587–599.

White,J.M. and Wilson I.A. (1987) *J. Cell Biol.*, **105**, 2887–2896.

Wiley,D.C. and Skehel,J.J. (1987) *Annu. Rev. Biochem.*, **56**, 365–394.

Wilson,I.A., Skehel,J.J. and Wiley,D.C. (1981) *Nature*, **289**, 368–373.

Wrigley,N.G., Brown,E.B., Daniels,R.S., Douglas,A.R., Skehel,J.J. and Wiley,D.C. (1983a) *Virology*, **131**, 308–314.

Wrigley,N.G., Brown,E.B. and Chillingworth,R.K. (1983b) *J. Microsc.*, **130**, 225–232.

Wrigley,N.G., Brown,E.B. and Skehel,J.J. (1986) In Harris,J.R. and Horne,R.W. (eds), *Electron Microscopy of Proteins, Volume 5: Viral Structure.* Academic Press, London, pp. 103–164.

Yewdell,J.W., Gerhard,W. and Bachi,T. (1983) *J.Virol.*, **48**, 239–248.

Received on September 20, 1994